Atmospheric Environment 139 (2016) 20–29

Contents lists available at ScienceDirect

Atmospheric Environment

journal homepage: www.elsevier.com/locate/atmosenv

Ultrafine particle size as a tracer for aircraft turbine emissions

Erin A. Riley [a], Timothy Gould [b], Kris Hartin [a], Scott A. Fruin [c], Christopher D. Simpson [a], Michael G. Yost [a], Timothy Larson [a, b, *]

[a] University of Washington, Department of Environmental and Occupational Health Sciences, Box 357234, Seattle, WA, 98198, United States
[b] University of Washington, Department of Civil & Environmental Engineering, Box 352700, Seattle, WA, 98198, United States
[c] University of Southern California, Keck School of Medicine, SSB 225F, MC 9237, 2001 N Soto Street, Los Angeles, CA, 90032, United States

HIGHLIGHTS

- Spatial measurements of ultrafine particle number (PN) and diameter in two cities.
- PN concentrations more than 5 km from airport are similar to those on freeways.
- Spatial distribution of mean ultrafine particle diameter is distinct near airport.
- Ratio of PN to black carbon is higher beneath approach path than elsewhere.

GRAPHICAL ABSTRACT

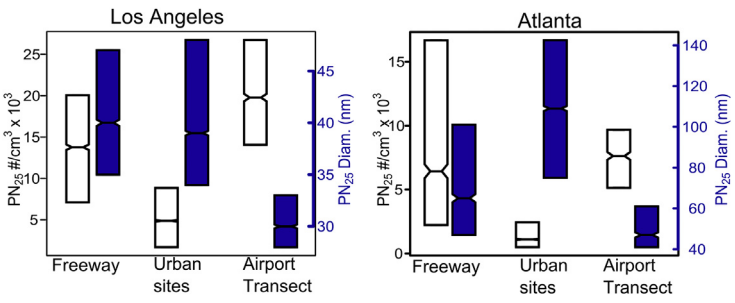

ARTICLE INFO

Article history:
Received 13 January 2016
Received in revised form
6 May 2016
Accepted 8 May 2016
Available online 10 May 2016

Keywords:
Ultrafine particles
Airport emissions
Mobile monitoring
Ultrafine particle size
Black carbon
Nitrogen dioxide

ABSTRACT

Ultrafine particle number (UFPN) and size distributions, black carbon, and nitrogen dioxide concentrations were measured downwind of two of the busiest airports in the world, Los Angeles International Airport (LAX) and Hartsfield-Jackson International Airport (ATL – Atlanta, GA) using a mobile monitoring platform. Transects were located between 5 km and 10 km from the ATL and LAX airports. In addition, measurements were taken at 43 additional urban neighborhood locations in each city and on freeways. We found a 3–5 fold increase in UFPN concentrations in transects under the landing approach path to both airports relative to surrounding urban areas with similar ground traffic characteristics. The latter UFPN concentrations measured were distinct in size distributional properties from both freeways and across urban neighborhoods, clearly indicating different sources. Elevated concentrations of Black Carbon (BC) and NO_2 were also observed on airport transects, and the corresponding pattern of elevated BC was consistent with the observed excess UFPN concentrations relative to other urban locations.

1. Introduction

The largest impacts of jet engine emissions on neighboring residential areas has until recently been thought to be primarily limited to areas within about a kilometer of edge of the runway. Characterization of air pollutants from aircraft traffic and airport activity has been primarily conducted at fixed sites located within 2 km of the airport runways (Carslaw et al., 2006; Hsu et al., 2013; Hu et al., 2009; Lai et al., 2013; Lobo et al., 2012; Masiol and Harrison, 2014, 2015; Westerdahl et al., 2008; Zhu et al., 2011) but mobile monitoring has also been used to confirm the area-wide impact of emissions from airport activities on near-airport neighborhoods within a few kilometers (Choi et al., 2013; Hsu et al.,

* Corresponding author. University of Washington, Department of Civil & Environmental Engineering, Box 352700, Seattle, WA, 98198, United States.
E-mail address: tlarson@u.washington.edu (T. Larson).

http://dx.doi.org/10.1016/j.atmosenv.2016.05.016
1352-2310/

2014). Recently, a mobile monitoring campaign was conducted in the approach path of LAX where a spatially dense sampling scheme uncovered a much larger area of impact covering 60 km^2 and extending 20 km downwind from the airport, the largest monitoring area effort to date (Hudda et al., 2014). The authors reported increased ultrafine particle number concentrations (UFPN) of 4–5 times normal at distances of 8–10 km from the airport on multiple independent days of sampling. Subsequently, fixed-site downwind measurements conducted at Schiphol airport in the Netherlands and supported by Gaussian plume models have shown substantial impacts of airport emissions on UFPN concentration extending >8 km from the airport (Keuken et al., 2015). With its ability to cover large areas, mobile monitoring may be the most effective means to refine the current understanding of the impact that aircraft (and airport) emissions have on air quality in a variety of urban settings.

Here we present an analysis that uses mobile monitoring data from Atlanta, GA and Los Angeles, CA to compare the spatial distributions of ultrafine particle metrics derived from three different mobile sampling strategies: downwind airport transects perpendicular to flight paths, on-road highway routes, and repeated measures at fuzzy points (neighborhood sampling centered on an intersection and utilizing a clover leaf approach to include all upwind and downwind conditions). This wide area approach provided a novel verification of the wide area impacts found by Hudda et al. (2014), and demonstrated the relatively high UFPN impacts of airports compared to freeways, which are usually considered to dominate UFPN concentrations in most urban areas in the U.S.

2. Methods

Ultrafine particle metrics included: PN_{10} (in Los Angeles only; UFPN, diameter > 10 nm), PN_{25} (UFPN, diameter > 25 nm), PN_{50} (UFPN, diameter > 50 nm), Dp_N (mean number diameter from PN_{25} measurement), and the ratio of PN_{25}/PN_{50}. We also simultaneously measured nitrogen dioxide (NO_2) and black carbon (BC). Instruments and their reporting limits are listed shown in Table 1. Instruments were checked or calibrated for zero and span (NO_2 analyzer) in the field periodically. Particle number instruments were previously evaluated by traceable methods at their respective manufacturers: the P-Trak was certified in May 2011 measuring a particle count that averaged 100.4% of test standard particle counts determined by a TSI 3080 Electrostatic Classifier and two TSI 3010 Condensation Particle Counters, and the NanoCheck 1.320 was equipped with a new aerosol detector by the manufacturer Grimm Technologies which confirmed the device to be working within specifications on July 30, 2012. More detailed discussion of the mobile platform can be found in the supplemental material.

Downwind airport transects were selected along residential neighborhood streets to minimize the impact of roadway traffic on the observations. The transects are expected to have distributions of traffic related air pollutant (TRAP) concentrations similar to the distributions captured by the fuzzy point (FP) monitoring, which were located on both high and low traffic-impacted roads. In LA, the transect locations were within the sampling area previously reported by Hudda et al. (2014), where a raster-pattern sampling scheme was used to detect a gradient in the 5th percentile of rolling 1 s UFPN measurements (over 30 s intervals) beneath the approach path of aircraft compared to adjacent neighborhoods. Finally, highway monitoring was meant to capture TRAP concentrations and characteristics associated with the most trafficked roadways in these cities. The comparison between the results of these three sampling strategies allowed us to investigate whether neighborhoods downwind of airports experience different air pollutant impacts compared to other urban locations that encompass a distribution of TRAP impacts.

2.1. Sampling methodology

Sampling consisted of highway, airport transect, and FP monitoring. FP locations were clusters of data ~600 m across, composed of a clover leaf pattern that produces more robust average and distributional concentrations of a given location by including all directions and orientations to surrounding traffic (Larson et al., 2009). We therefore define the term 'fuzzy point' or "FP," to include data points encompassed within a circle 300 m in radius centered on a given intersection. For each FP we obtained mobile data at 10 s resolution for a total of ~6–10 min during each transit, thus, the mobile monitor captures a distribution of values assigned to this location. FPs are selected in residential urban neighborhoods encompassing a range of traffic characteristics from low traffic residential streets, to arterials with mixed traffic composition, to near highway locations (see Figs. 1 and 2). The 43 FPs were divided among three routes, with the airport transects and highway sampling comprising the fourth route. Routes were driven 3–4 times, with the order of sites visited reversed in direction for successive transits through each route.

Sampling in Los Angeles took place between June 14th, 2013 and July 1st, 2013 and was divided into four routes with one route driven per day between the hours of 12:00–19:00 local time. Airport transects and freeways were sampled on June 22nd, 27th, and July 1st and an additional day of highway-only driving was performed June 14th. Sampling in Atlanta took place during a shorter time period between the 8th and 17th of September 2013 with airport transects sampled on September 9th, 11th, 13th, 14th, and 17th. The complete sampling space for the LAX and Atlanta campaigns is depicted in Figs. 1 and 2. Highway sampling in Atlanta took place on September 10th and 15th; highway sampling data were more limited in spatial extent in Atlanta than in LA because it was not a design priority for the former campaign. In Atlanta additional highway data were selected manually by defining a polygon around the urban-center highways in Google Earth; points within the polygon were added to the highway sampling data set in Atlanta from the remaining sampling days. FP sampling in Atlanta

Table 1
Mobile platform instrumentation.

Parameter	Instrument	Manufacturer	Measurement range
PN_{25} concentration and mean diameter (25–400 nm)	NanoCheck 1.320	GRIMM	$0–4 \times 10^6$ particles/cm^3
PN_{50} number concentration (50–1000 nm)[a]	P-Trak 8525, with particle diffusion screens	TSI	$0–5 \times 10^5$ particles/cm^3
PN_{10} number concentration (10–1000 nm) (Los Angeles only)	CPC model 3007 (ethanol based)	TSI	$0–1 \times 10^5$ particles/cm^3
Black carbon (BC)	Micro-Aethalometer AE52[b]	AethLabs	0–1 mg/m^3
NO_2	Cavity Attenuated Phase Shift (CAPS) monitor	Aerodyne Research	0.1–3000 ppb
Positioning & real-time tracking	GPS Receiver BU-353	US GlobalSat	10 m accuracy

[a] Normal P-Trak lower size limit without screen is 20 nm, the screen captures 20–50 nm particles by diffusion to provide additional independent size resolved count data.
[b] MicroAeth® Model AE51, custom modified by AethLabs for dual wavelength acquisition.

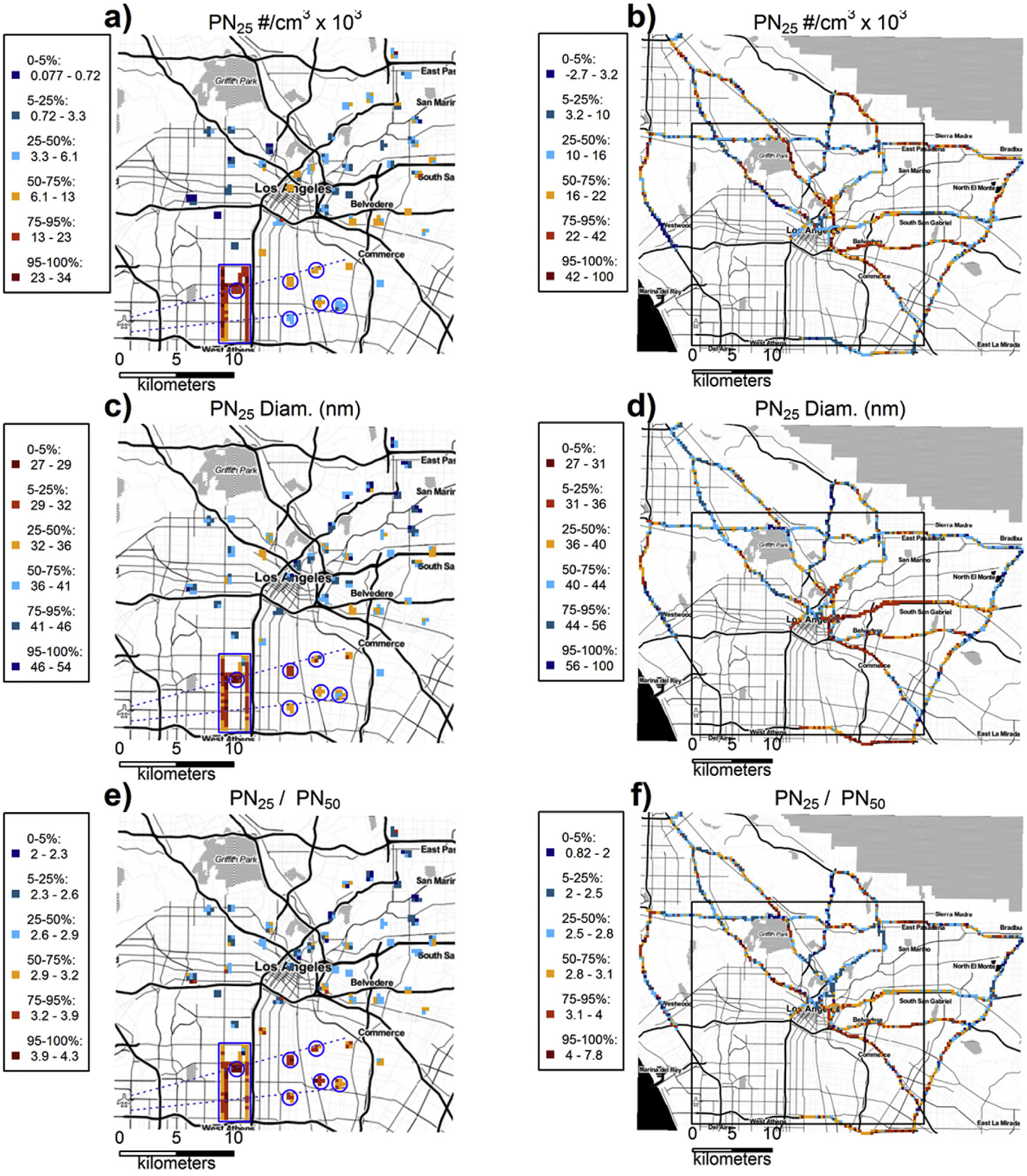

Fig. 1. Map of Los Angeles mobile monitoring data for three pollutant metrics. Data were spatially binned into a grid with 300 m × 300 m cell size, and the median was calculated for each bin. Color scale represents quantiles of the resultant spatial bins. Original PN_{25} concentrations have been adjusted by aligning data collected on separate days using the daily 5th percentile. PN_{25} concentrations presented are the incremental concentration change from the 5th percentile; there are no negative measurements in the original data. Particle size and PN_{25}/PN_{50} are calculated with the original (unaligned) data. Figures a,c, and e: The solid blue box encloses the airport transects, solid blue circles indicate airport FPs. Dashed blue lines leading to LAX airport indicate approximate approach paths to the two landing strips (see supplemental Figure S2). Figures b,d, and f: The black box indicates the zoomed-in spatial region displayed in Figures a,c, and e.

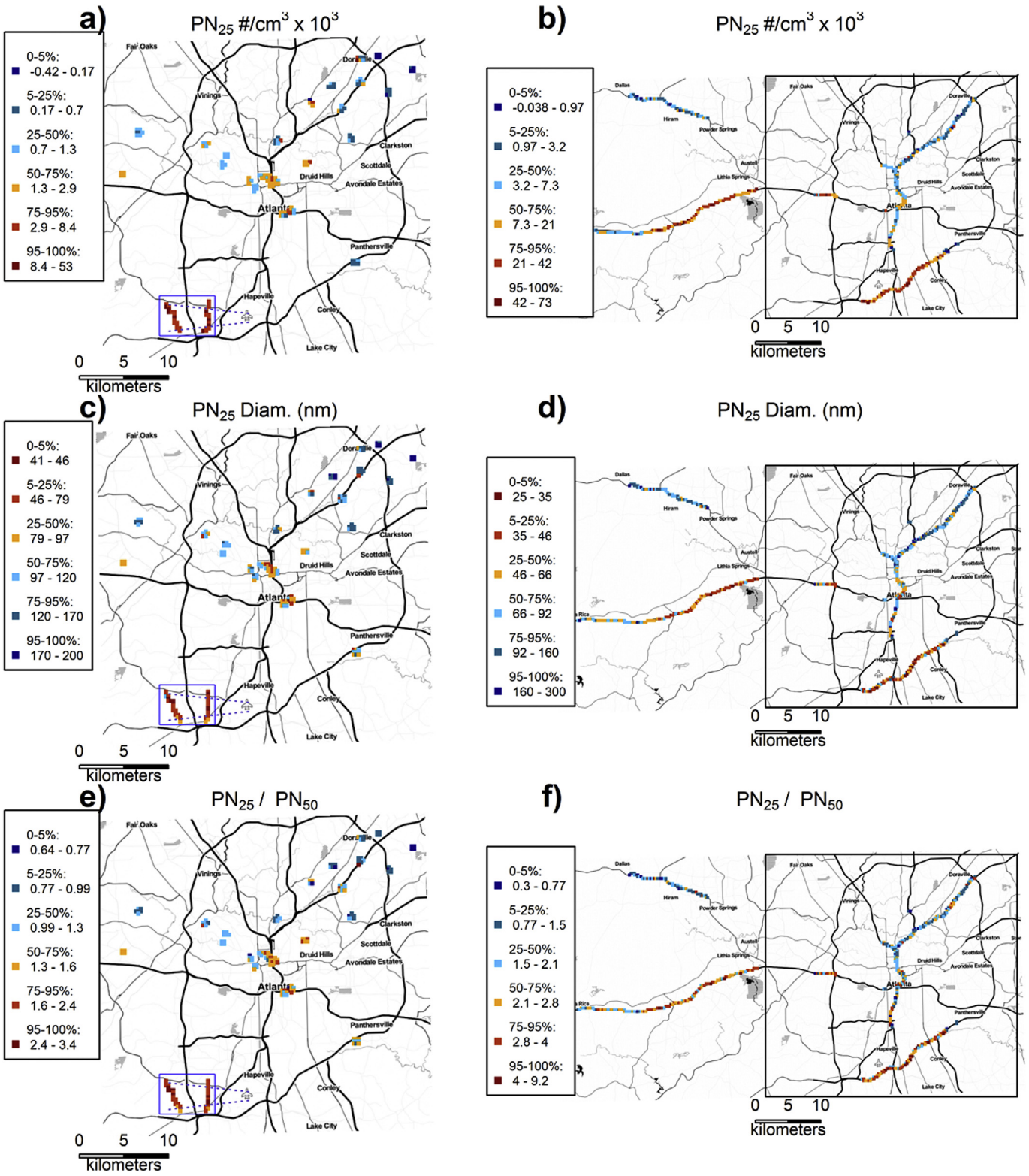

Fig. 2. Map of Atlanta mobile monitoring data for three pollutant metrics. Data were spatially binned into a grid with 300 m × 300 m cell size, and the median was calculated for each bin. Color scale represents quantiles of the resultant spatial bins. Original PN_{25} concentrations have been adjusted by aligning data collected on separate days using the daily 5th percentile. PN_{25} concentrations presented are the incremental concentration change from the 5th percentile; there are no negative measurements in the original data. Particle size and PN_{25}/PN_{50} are calculated with the original (unaligned) data Figures a,c, and e: The solid blue box encloses the airport transects and the dashed blue lines leading to ATL airport indicate approximate approach paths to the two landing strips (see supplemental Figure S3). Figures b,d, and f: The black box indicates the zoomed-in spatial region displayed in Figures a,c, and e.

consisted of overlapping clusters of FPs arrayed in a gradient at increasing distance from freeways along with 20 dispersed FPs. The spatial extent of the FP, highway, and airport transect data can been seen in Fig. 2. For both cities the airport transects consisted of low traffic residential roadways that were selected to minimize the impact from mobile sources. Maps of the airport transect data are provided in the supplemental material (Fig. S1). A detailed description of the methods for sample collection, sample analysis and statistical treatment of the data can be found in the supplemental material.

2.2. Mobile platform temporal adjustments

A central challenge to the use of mobile monitoring data for spatial analysis is adjusting for (or removing) temporally-varying background contributions to the measurements, such as day to day differences in meteorology that affect the entire region. For this analysis we derived distributional properties (e.g. 5th, 25th, 50th, 75th and 95th percentiles) of the pollutant concentrations measured by the mobile platform. To allow more direct comparisons across locations, between-day temporal trends were accounted for by aligning the data to the daily 5th percentile concentrations. The 5th percentiles tend to reflect regionally consistent concentrations when no localized source contributions are present. We use this value as an "estimated urban background". This adjustment was particularly important since the locations were sampled on different days (refer to supplementary material for additional details and sensitivity tests). The daily 5th percentile was first calculated from all available mobile platform data, including time periods when the platform was in transit between selected sites and then subtracted from all the measurements. The two exceptions involved variables other than concentration where the 5th percentile does not necessarily represent an urban background, specifically the measured mean particle diameter and PN_{25}/PN_{50}.

2.3. Map generation

After the data were aligned to the daily 5th percentile, we then excluded measurements that were collected between sampling locations. Maps of LA and Atlanta were obtained using the package "OpenStreetMap" in R and then both maps and data were projected to UTM coordinates (Fellows and Stotz, 2013). The data were then spatially binned by calculating the median along a grid with cell size 300 m $\times$ 300 m using the R package "Raster" (Hijmans, 2015). This gridding results in multiple grid cell values per FP (~4–9) depending upon how the data defined by the 300 m radius overlap the spatial grid. The median is less sensitive than the mean to the presence of discrete plumes in the distribution of concentrations measured at a location. Quantiles of spatial-grid cells values were calculated for each map and were used to generate the color axis.

3. Results

3.1. UFPN maps

The extent of the mobile monitoring campaign in Los Angeles is indicated in Fig. 1a–f. Fig. 1a shows elevated PN_{25} at FPs beneath the LAX approach paths (dotted lines) relative to FPs at mixed traffic/residential locations (the detailed landing approach patterns for LAX and ATL airports are provided in the supplemental material, Figs. S2 and S3). The concentrations near the airport generally exceed the 75th percentile of all non-freeway measurements, but are about half the on-freeway concentrations in the same quantile (Fig. 1a–b). The smallest 25th percentile (<30 nm) of PN_{25} count mean diameter observed in Los Angeles occurs in neighborhoods beneath the aircraft approach path. The ratio of PN_{25}/PN_{50} shows a similar spatial pattern, where the airport jet pathway and airport FPs (enclosed by 6 blue circles in –Fig. 1a and c) all have percentiles above 75%, corresponding to a prevalence of smaller diameter particles in this location compared to both the freeway and FP locations.

The spatial extent of the Atlanta campaign is shown in Fig. 2a–f. As in Los Angeles, elevated concentrations of PN_{25} were measured along the near airport transects relative to the FP sampling (Fig. 2a) but the highest PN_{25} concentrations were observed on the freeways (Fig. 2b). Particle diameters in the airport transect were in the smallest 25th percentile (<60 nm) near the ATL airport; whereas FP locations were primarily in the larger 50th percentile (>90 nm). In Atlanta the smallest diameter particles (<40 nm) were measured on the freeways, and were similar in diameter to those measured on LA freeways (30–45 nm). We measured larger particle diameters overall in Atlanta relative to LA. The ratio of PN_{25}/PN_{50} showed similar patterns to the particle sizes with the largest ratios occurring near the airport and on freeways, indicating a prevalence of smaller diameter particle sizes.

We additionally examined the choice of the median to represent the PN_{25} concentrations within the spatial bins. The median should be less prone to vehicle exhaust plumes but may still be influenced by traffic. Hudda et al. (2014) made spatial comparisons of 1 s UFPN data using the 5th percentile. We find the same spatial pattern in PN_{25} using the 5th percentile as the parameter for spatial binning as we did using the median (see Fig. S4 in the supplemental information). The concentrations calculated based upon the 5th percentile in the airport transects are still largely in excess of the "estimated urban background" (75th–95th quantiles: 7–14 $\times$ 10^3 #/cm^3 above background for LA). These concentrations are a much larger incremental increase in particle concentrations compared to the FPs (median: 1.6 $\times$ 10^3 #/cm^3 above background for LA).

3.2. Boxplot comparisons

After the data were aligned to the daily 5th percentile ("estimated urban background") the 10 s data were then assigned to categories: Airport transect, FPs, and freeway. We created an additional category of airport-FPs for Los Angeles (indicated by blue circles in Fig. 1). These airport FPs were classified based upon the LAX noise monitoring locations, aircraft traffic data (see Supplemental material Fig. S2), and the ultrafine particle plume reported by Hudda et al. (2014) which all indicated that six FPs are likely within the LAX impact region.

Boxplots of NO_2, BC, PN_{25} (diameter 25–400 nm), PN_{50} (diameter 50–1000 nm), D_{pN} (count mean diameter), and the ratio of PN_{25}/PN_{50} are provided in Figs. 3 and 4 a–f for the data categories. The concentrations of NO_2, BC, PN_{25}, and PN_{50} are differential relative to the "estimated urban background", a consequence of the daily temporal adjustment. There are no negative measurements in the original data. The total number of 10 s observations for each pollutant metric by category is provided at the top of each boxplot. Hartsfield-Jackson Atlanta International Airport (ATL) sampling dates occurred during easterly flows except for 9/13/2013. This date was excluded from the boxplot analysis so that all the data reported here correspond to the easterly landing approach of aircraft.

Comparisons of the four data categories for Los Angeles are depicted in Fig. 3a–f. Fig. 3a shows that the PN_{25} concentrations observed along the airport transects exceed those observed broadly across the LA freeway system. This is not true for PN_{50}, where airport concentrations are similar to those observed on freeways (Fig. 3b). However, both PN_{50} and PN_{25} in the airport transect far exceed the distributions observed at FPs by factors of three and

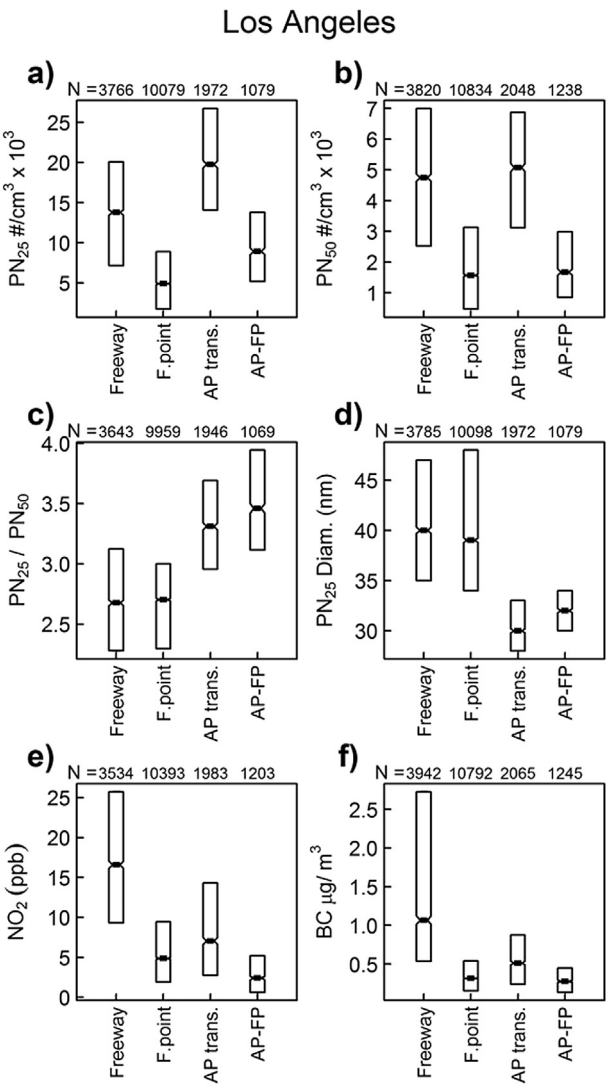

Fig. 3. Boxplots of the 25th, 50th, and 75th percentiles for select pollutants measured within the data designations defined in Fig. 1 for LA. Abbreviations: F.point (fuzzy point), AP trans. (airport transect), AP-FP (airport fuzzy point). Pollutant concentrations are incremental departures from the 5th percentile, except for PN_{25}/PN_{50} ratio and particle size data which are determined from the original (unaligned) data (see data adjustment in methods). Number of 10 s observations contributing to each boxplot is listed above each figure. Notches are ± 1.58 (interquartile-range)/sqrt(n), and provide an approximate 95% confidence that two medians differ if the notches do not overlap.

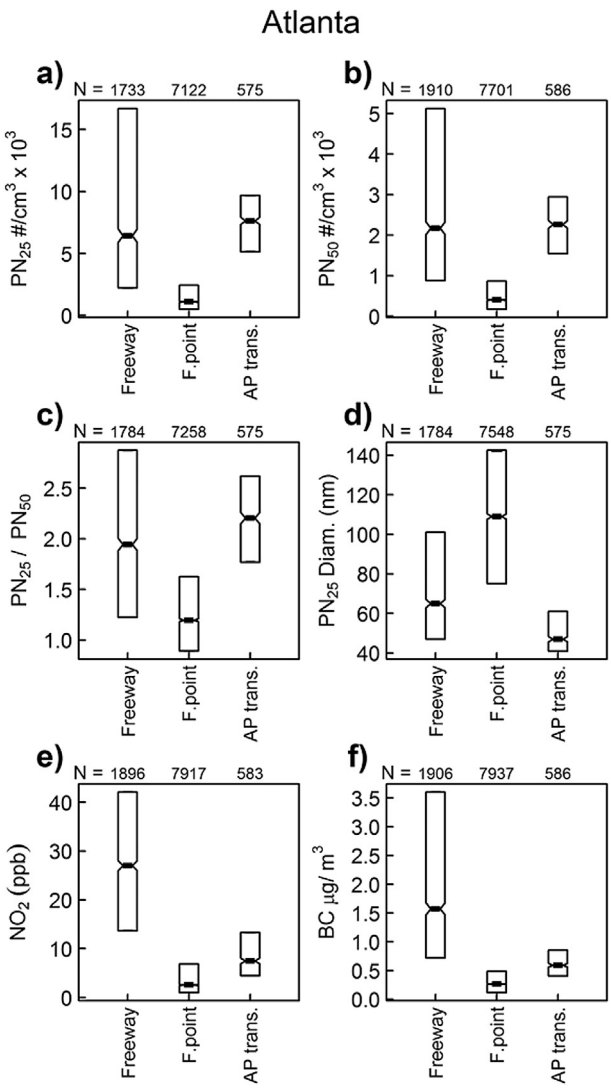

Fig. 4. Boxplots of the 25th, 50th, and 75th percentiles for select pollutants measured within the data designations defined in Fig. 2 for Atlanta. Abbreviations: F.point (fuzzy point) and AP trans. (airport transect). Pollutant concentrations are departures from the 5th percentile except for PN_{25}/PN_{50} ratio and particle size data which are determined from the original (unaligned) data (see data adjustment in methods). Number of 10 s observations contributing to each boxplot is listed above each figure. Notches are ± 1.58 (interquartile-range)/sqrt(n), and provide an approximate 95% confidence that two medians differ if the notches do not overlap.

four, respectively. Fig. 3c shows the ratio of PN_{25}/PN_{50} for the airport transect and airport-FPs are also distinct from both freeway and FPs. Fig. 3d shows that airport transects have distinctly smaller particle sizes compared to those of both freeways and FPs. The NO_2 and BC concentrations are much higher on the freeways than in the neighborhood locations. The airport transects have slightly higher NO_2 and BC concentrations than the FPs and airport-FPs.

In Atlanta the PN_{25} and PN_{50} concentrations are highest on the freeways. As in LA, the PN_{25} and PN_{50} concentrations observed in the airport transects far exceed the distribution of concentrations observed in FPs. In Atlanta, the count mean particle size measured at FPs are much larger than at the other two location categories. In contrast, the distributions of particle sizes on freeways and FPs were similar in LA. Similar to LA, the spatial distribution of count mean particle sizes along airport transects is narrower than the other two location categories, and has a smaller median diameter. The spatial distribution of count mean particle size along the airport transects is not as narrow as observed in LA, with a comparatively larger median particle diameter (47 nm compared to 30 nm in LA). The ratio of PN_{25}/PN_{50} is similar on freeways and along airport transects, unlike what was observed in LA. Finally, the concentrations of NO_2 and BC in Atlanta were similar to what is seen in LA.

In Los Angeles we had an additional particle sizing instrument with a 10 nm lower cut-off for two of the sampling days. A comparison of the time series of this instrument with the other particle instruments for one day of airport transect monitoring is shown in Fig. 5. This instrument recorded similar concentrations to those measured by the instrument with a 25 nm lower cut-off.

4. Discussion

The elevated concentrations of UFPN (measured as PN_{25}) in the

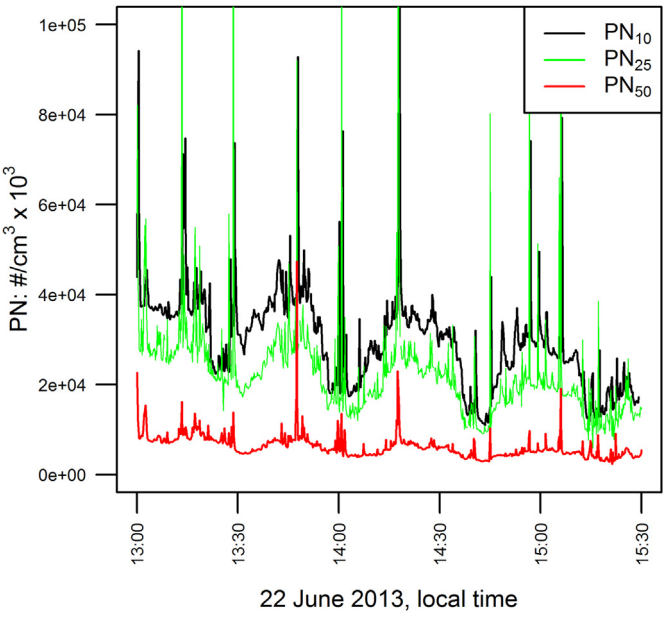

Fig. 5. Time series of unadjusted data during the airport transect sampling on June 22, 2013. An additional particle counter was included on this day with a lower size limit of detection of 10 nm and was only operated for the airport transect (black line).

aircraft approach path of LAX as shown in Fig. 1a confirm the findings reported by Hudda et al. (2014) of large areas of highly elevated particle number concentrations beneath the incoming flight paths. We additionally found that the median and interquartile range of the spatial distribution of UFPN particle sizes measured downwind of the airport are distinctly smaller and narrower than those measured at locations with known traffic-related sources of UFPN (i.e. the freeways). The freeway and fuzzy point data provide a useful benchmark for the expected distribution of particle sizes resulting from convolved sources of mixed traffic including differences in vehicle type (i.e. light duty passenger, diesel trucks etc), vehicle speed, engine age, engine loads, and fuel composition. These factors affect the size distributions of ultrafine particles significantly (geometric mean diameter spanning 10 nm–100 nm) as has been discussed in a recent review (Vu et al., 2015); therefore in an urban setting we would expect variability in the spatial distribution of mean particle diameter. Evidence for this can be seen in Figs. 1 and 2 c, where individual fuzzy points exhibit more than one quantile of mean particle diameter, and also in Figs. 3 and 4 d where the interquartile ranges of all fuzzy points and highways are similar.

The smaller interquartile range of mean particle diameter, and smaller overall mean diameter in the airport transects compared to fuzzy points indicates that ultrafine particles in the LAX approach path have a different primary source other than car and truck traffic, presumably aircraft. The smaller count mean size of these ultrafine particles can be observed in both the direct measurement of particle sizes and in the ratio of the two UFPN instruments with different lower size thresholds (see Fig. 3). Smaller particle count mean diameters were also observed in the near-airport neighborhood in Atlanta (see Fig. 2) especially compared to other urban neighborhood locations (see Figs. 2 and 4). These boxplots clearly demonstrate that the count mean particle size is a much better tracer of the aircraft plume than either PN_{25} and PN_{50} alone. These findings suggest that particle sizing is a useful tool for differentially detecting ground-level aircraft related ultrafine particles from those generated by vehicle traffic in urban areas.

The peaks in particle number for the 10 nm and 25 nm cut-off instruments shown in Fig. 5 correspond to passing underneath the LAX flight path. Similar peaks are less clearly present for particle number >50 nm, a particle size range that is more associated with urban vehicle traffic and not aircraft emissions in urban areas. The similar intensity of the PN_{10} and PN_{25} instruments is consistent with particle sizes in the range 10–20 nm associated with low-thrust conditions of aircraft (Kinsey, 2009; Lobo et al., 2012). UFPN size distributions were recently measured near LAX using a combination of stationary and mobile monitoring beneath the descent paths of landing aircraft, including the UFPN spikes that corresponded to the landing of individual jets within 3 km of the airport. (Hudda and Fruin, 2016). They found a bimodal distribution with a primary mode of <20 nm, and a secondary mode at ~65 nm. Similar bimodal distributions were reported by Lobo et al. at the runway of Oakland international airport. (Lobo et al., 2012). Hudda and Fruin (2016) also reported Los Angeles urban background ultrafine particle sizes between 25 and 50 nm, consistent with our findings.

The boxplot comparison of the airport transects, FPs, and freeway TRAP distributions show that airport transects also have elevated levels of NO_2 and BC relative to what is observed in neighborhoods citywide for both Atlanta and Los Angeles. These elevated concentrations may result from the combination of both incoming jet emissions as well as the downwind transport of jet idling and takeoffs, with the latter known to be relatively high in BC and NOx. As air-traffic increases, concerns have been raised regarding advection of pollutants from increased roadway traffic and airport ground activities into nearby neighborhoods. Measurements in neighborhoods adjacent to a medium-sized airport (T.F. Green International Airport in Warwick, RI, USA), showed that the ultrafine impact from the edge of runway decayed 3-fold within 500 m (Hsu et al., 2014). This is similar to what is observed on highways. Annual Average Daily Traffic (AADT) data available from the California and Georgia departments of Transportation show that vehicle traffic near LAX and ATL airports are not the highest in either urban area, nor is there a remarkable percentage of truck traffic near those airports, especially compared to freight intensive areas (i.e. the port) (see Figs. S5–S8 in the supplemental material). Near-road gradient measurements taken as part of our quality assurance plan for mobile monitoring show a decay to background for PN, BC, and NO_2 within 500 m downwind of major freeways in the city center (I-10 in LA and I-85 in Atlanta) with AADT exceeding 230,000 in both cities (see Figs. S9–S11 in the supplemental material). This sub-kilometer distance-decay of traffic-related pollutants has been well established by ourselves and others, see (Riley et al., 2014) and references therein. Measurements in each city's center (Figs. 1 and 2) show that ultrafine particle levels are elevated relative to less trafficked areas; however, they do not exceed what is observed on both freeways and along the downwind airport transects. Downwind transport and dispersion of pollutants from ground-level activities at airports requires further investigation; however, as others have suggested the concentrations observed in the airport transects are likely partly attributable to downward transport of aircraft emissions (Hudda and Fruin, 2016; Hudda et al., 2014).

While ground-emissions disperse horizontally and are carried downwind, a major source of dispersion and dilution of emissions is vertical mixing with surrounding air. Our measurements were conducted in the afternoon when the convective boundary layer motions are pronounced. From a height of 500 m (such as the height of aircraft above our monitoring transects in LA) a parcel of air would reach the surface boundary layer within 3–8 min. In addition to vertical transport of pollutants due to surface heating, wake vortices generated by the rapid movement of air across the aircraft wings entrain engine emissions and rapidly descend before

Table 2
Median UFPN and BC concentrations in fuzzy points and airport transects and calculated expected excess UFPN.

Variable	Los Angeles			Atlanta		
	F.P.	Airport	Excess	F.P.	Airport	Excess
[a]C_m (ng/m^3)	318	514	196	269	594	325
ρ (g/cm^3)	–	–	1[c]	–	–	1[c]
d (nm)	39	30	30[b]	120	47	47[b]
C_N (#/cm^3)	4890	19,800	14,900	1100	7630	6530
$\widehat{C}_N$(#/cm^3)	–	–	13,900	–	–	5980

[a] Black Carbon mass concentration.
[b] Diameter directly used from airport transect measurements.
[c] From Durdina et al., 2014.

horizontally dispersing. The dispersion of jet engine exhaust as a result of the vortices has been studied at cruise conditions (Unterstrasser et al., 2014). In their model, jet engine exhaust initially becomes entrained and rapidly diluted by the forming pair of vortices. The vortices then transport the entrained exhaust downwards before the vortices break up and dissipate. The initial decent rate of the vortex pair is 1.5 m/s; after approximately 3 min, the emissions become detrained and the downward vertical displacement of the plume has reached ~450 m, with a vertical span of about the same. Further research is needed to understand how take-off and landing aircraft emissions arrive and disperse at ground level from different release heights.

Reports on the composition of jet engine exhaust show ultrafine particle size distributions that are dominated by soot particles in the range of 10–40 nm (Kumar et al., 2013; Liati et al., 2014). Nucleation mode particles are also present in exhaust and form when sulfonated and organic gases in the concentrated plume condense and subsequently aggregate. Due to rapid dilution of the plume (see discussion above), aging processes for aircraft exhaust are expected to be similar to those from ground sources. Approximately 80% of PN in the form of secondary aerosols are generated in the initial period that the plume is still concentrated; the composition of primary and secondary aerosols have been measured in advected plumes at both Oakland international and ATL airports proximate to the runway (Lobo et al., 2012, 2015). Other particle growth processes such as aggregation and photo-catalytic aging occur on longer time-scales (i.e. hours) (Payne et al., 2014). Ultimately, the ambient ultrafine particle size distribution evolves depending upon the composition of exhaust (a function of fuel composition and engine thrust) and ambient levels of condensates (Starik et al., 2013; Timko et al., 2013) which could account for the differences in PN_{25} particle sizes we observe comparing LA and Atlanta FPs (39 nm and 120 nm, respectively). What we can infer from the studies available is that Atlanta has the potential for particle growth from both biogenic sources (isoprene) in the summer and elevated ambient SO_2 concentrations, which would not be the case for coastal Los Angeles. (Hatch et al., 2011; Payne et al., 2014; Woo et al., 2001). Although the observed systematic differences in ultrafine particle sizes between Los Angeles and Atlanta are interesting, they are complex, and beyond the scope of this work. However, in both cities the average ultrafine particle size near the airport is less than in other locations within the urban area.

Measurements of particulate matter density from jet engine exhaust show that soot particles have near unit density 1 g/cm^3 (Durdina et al., 2014). Another study of aircraft particulate matter reported primary emission of black carbon particles of varying size (13–24 nm) depending upon engine operating characteristics (Liati et al., 2014). As a first order estimate assuming pure spherical carbon particles, we estimated the expected UFPN in the airport transects given the excess BC mass concentration observed (calculated as median airport transect minus median FP), assuming the measured median PN_{25} particle diameter in the airport transects, and with the following first order approximation:

$$\widehat{C}_N = C_m \left[\frac{\pi \rho d_{\overline{m}}^3}{6}\right]^{-1}$$

where $\widehat{C_N}$ is the estimated number concentration, C_m is the mass concentration, ρ is the particle density, and $d_{\overline{m}}$ is the mean diameter. The input parameters and results are provided in Table 2, which shows a ~7% underestimation of the observed excess PN_{25} in both cities. If the excess PN_{25} is indeed BC from aircraft, then 38% of the BC measured in the airport transects in LA can be attributed to aircraft emissions at ~10 km from the airport and 55% of the BC measured in airport transects in Atlanta at ~5 km from the airport (see Table 2 and Figs. 3 and 4).

The amount of black carbon observed in the airport transects is

Table 3
Emission indices for mobile sources.

Source	Fleet year/type	PN 10^{14} particles/kg fuel	BC mg/kg fuel	PN/BC (#/mg)	Reference
Aircraft	B737-700 (30% power)	63.7 ± 3.7	110 ± 57	5.8×10^{13}	APEX report Tables E1 and G1. (Kinsey, 2009)[a]
	B737-300 (30% power)	33.4 ± 3.4	250 ± 47	1.3×10^{13}	
	LEAR 25 (30% power)	110 ± 10	302 ± 27	3.6×10^{13}	
	ENB145 (30% power)	42 ± 26	23.4 ± 23	1.8×10^{14}	
	A300 (30% power)	80.2 ± 7	35 ± 26	2.3×10^{14}	
	B757 (30% power)	40 ± 18	229 ± 76	1.7×10^{13}	
	B737-700 (85% power)	7.3 ± 2.5	405 ± 103	1.8×10^{12}	
	B737-300 (85% power)	60 ± 26	710 ± 102	8.4×10^{12}	
	LEAR 25 (85% power)	79 ± 24	784 ± 203	1.1×10^{13}	
	ENB145 (85% power)	34 ± 15	147 ± 43	2.3×10^{13}	
	A300 (85% power)	20.7 ± 3.6	385 ± 66	5.3×10^{12}	
	B757 (85% power)	11 ± 3	873 ± 190	1.2×10^{12}	
HD diesel	2013 drayage	24.7 ± 4.8	280 ± 50	8.8×10^{12}	(Preble et al., 2015)
	2013 drayage (no particle filter)	47.2 ± 9.7	1110 ± 260	4.25×10^{12}	(Preble et al., 2015)
	2011 (Freeway use)	4.3 ± 1	54 ± 6	7.9×10^{12}	(Kozawa et al., 2014)
	2007 (cruise < 30 mph)	36	970	3.7×10^{12}	(Park et al., 2011)
	2007 (cruise > 30 mph)	14	220	6.4×10^{12}	(Park et al., 2011)
LD gasoline	2007 (cruise < 30 mph)	5.2	50	1.0×10^{13}	(Park et al., 2011)
	2007 (cruise > 30 mph)	5.5	90	6.1×10^{12}	(Park et al., 2011)

[a] Average and standard deviation calculated from the mean emission indices from multiple tests at each power for each aircraft. The indices without loss correction were used. HD = Heavy Duty, LD = Light Duty.

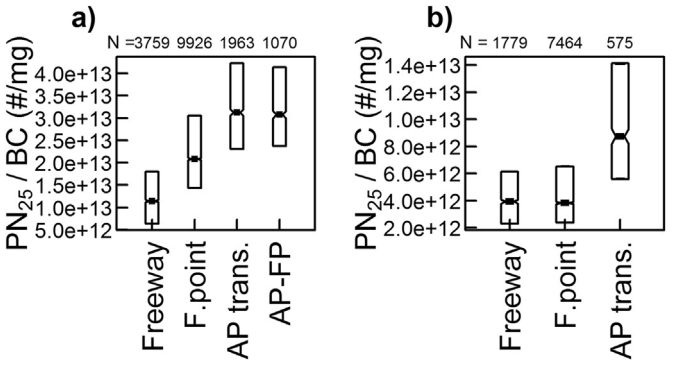

Fig. 6. The ratio of PN_{25}/BC for a) Los Angeles and b) Atlanta. Ratios are calculated on unaligned data (no daily adjustment). The same data designations are used as in Figs. 3 and 4. Number of 10 s observations contributing to each boxplot is listed above each figure. Notches are ± 1.58 (interquartile-range)/sqrt(n), and provide an approximate 95% confidence that two medians differ if the notches do not overlap.

still far less than what is observed on the freeways (see Figs. 3 and 4f). This is expected from the emission indices for BC and PN of aircraft jet-engine exhaust relative to heavy duty diesel and light duty vehicle exhaust. Recently reported emission indices for BC and PN for aircraft, light duty gasoline, and heavy duty diesel vehicles are provided in Table 3. Table 3 also shows emission index ratios for PN to BC. For aircraft at 30% power (landing approach power) the ratios span 2–23 × 10^{13} (#/mg) for various aircraft, whereas the ratios for heavy duty diesel and car traffic are all less than 10^{13}. Boxplots of the ratios of PN_{25}/BC (calculated from data without the daily data adjustment) are presented in Fig. 6. The figure shows that the ratio of PN_{25}/BC is observed to be higher in the airport transects in both cities consistent with the expected values from Table 3. Maps of the ratio of our observed PN_{25}/BC can be found in the supplemental material (Figs. S12 and S13).

This study is limited in duration and in scope (one campaign and sampling only in the afternoon) and therefore the observations are not generalizable to concentrations near these airports during all seasons and times of the day. However, these results help build a case for broader efforts in air pollution monitoring that extend >5 km from the airport and for the inclusion of ultrafine size-distribution metrics to aid in identifying the smaller soot particles from aircraft turbine exhaust relative to those from roadway traffic. Our efforts near LAX confirm the findings of Hudda et al. (2014), who found a 4-fold increase in UFPN concentrations compared to near airport locations at a similar distance from the airport as we did in this study. Our study also compared the airport monitoring to the larger city of LA, and shows that the monitoring regions below the LAX approach path have different particle size characteristics compared to similar neighborhoods in other areas of Los Angeles, including those near freeways. It would be of interest to have better spatial coverage to characterize both approach paths for ATL, the busiest airport in the USA. That being said, these mobile monitoring results are so far the first efforts at characterizing UFPN concentrations at >5 km distance from ATL.

5. Conclusions

UFPN concentrations under airport descent paths were found to be elevated in summer afternoon periods compared to typical urban neighborhoods in both Atlanta and Los Angeles. The ultrafine particles observed below the airport descent paths were distinct by being smaller in diameter than particles measured in other neighborhoods and freeways within the same city. Particle size may be a simple way to detect aircraft UFPN differentially from traffic related UFPN in near airport neighborhoods; this can be measured simply by using multiple particle count instruments employing different lower size thresholds. In addition the ratio of PN_{25}/BC is a way to connect the observed concentrations to known emission indexes which is a helpful assessment of the air pollution mix being measured by the mobile platform, and provides additional evidence for the impact of aircraft exhaust on urban UFPN near airports.

Acknowledgement

This publication was made possible by USEPA grant (RD-83479601-0). Its contents are solely the responsibility of the grantee and do not necessarily represent the official views of the USEPA. Further, USEPA does not endorse the purchase of any commercial products or services mentioned in the publication. Additional support provided by the National Institute of Environmental Health Sciences (T32ES015459, P30ES007033). This publication's contents are solely the responsibility of the authors and do not necessarily represent the official views of the sponsoring agencies. We'd also like to thank the Southeastern Center for Air Pollution and Epidemiology for logistical support of our monitoring efforts in Atlanta.

Appendix A. Supplementary data

Supplementary data related to this article can be found at http://dx.doi.org/10.1016/j.atmosenv.2016.05.016.

References

Carslaw, D.C., Beevers, S.D., Ropkins, K., Bell, M.C., 2006. Detecting and quantifying aircraft and other on-airport contributions to ambient nitrogen oxides in the vicinity of a large international airport. Atmos. Environ. 40 (28), 5424–5434.
Choi, W., Hu, S.S., He, M.L., Kozawa, K., Mara, S., Winer, A.M., Paulson, S.E., 2013. Neighborhood-scale air quality impacts of emissions from motor vehicles and aircraft. Atmos. Environ. 80, 310–321.
Durdina, L., Brem, B.T., Abegglen, M., Lobo, P., Rindlisbacher, T., Thomson, K.A., Smallwood, G.J., Hagen, D.E., Sierau, B., Wang, J., 2014. Determination of PM mass emissions from an aircraft turbine engine using particle effective density. Atmos. Environ. 99, 500–507.
Fellows, I., Stotz, J.P., 2013. OpenStreetMap, R Package Version 0.3.1. http://CRAN.R-project.org/package=OpenStreetMap.
Hatch, L.E., Creamean, J.M., Ault, A.P., Surratt, J.D., Chan, M.N., Seinfeld, J.H., Edgerton, E.S., Su, Y., Prather, K.A., 2011. Measurements of isoprene-derived organosulfates in ambient aerosols by aerosol time-of-flight mass spectrometry – Part 1: single particle atmospheric observations in Atlanta. Environ. Sci. Technol. 45 (12), 5105–5111.
Hijmans, R.J., 2015. Raster: Geographic Data Analysis and Modeling. R package version 2.3-40. http://CRAN.R-project.org/package=raster.
Hsu, H.H., Adamkiewicz, G., Houseman, E.A., Spengler, J.D., Levy, J.I., 2014. Using mobile monitoring to characterize roadway and aircraft contributions to ultrafine particle concentrations near a mid-sized airport. Atmos. Environ. 89, 688–695.
Hsu, H.H., Adamkiewicz, G., Houseman, E.A., Zarubiak, D., Spengler, J.D., Levy, J.I., 2013. Contributions of aircraft arrivals and departures to ultrafine particle counts near Los Angeles International Airport. Sci. Total Environ. 444, 347–355.
Hu, S., Fruin, S., Kozawa, K., Mara, S., Winer, A.M., Paulson, S.E., 2009. Aircraft emission impacts in a neighborhood adjacent to a general aviation airport in Southern California. Environ. Sci. Technol. 43 (21), 8039–8045.
Hudda, N., Fruin, S.A., 2016. International airport impacts to air quality: size and related properties of large increases in ultrafine particle number concentrations. Environ. Sci. Technol. 50 (7), 3362–3370.
Hudda, N., Gould, T., Hartin, K., Larson, T.V., Fruin, S.A., 2014. Emissions from an international airport increase particle number concentrations 4-fold at 10 km Downwind. Environ. Sci. Technol. 48 (12), 6628–6635.
Keuken, M.P., Moerman, M., Zandveld, P., Henzing, J.S., Hoek, G., 2015. Total and size-resolved particle number and black carbon concentrations in urban areas near Schiphol airport (the Netherlands). Atmos. Environ. 104, 132–142.
Kinsey, J.S., 2009. Characterization of Emissions from Commercial Aircraft Engines during the Aircraft Particle Emissions EXperiment (APEX) 1 to 3, EPA-600/R-09/130. United States Environmental Protection Agency, National Risk Management Research Laboratory: Research Triangle Park, NC.
Kozawa, K.H., Park, S.S., Mara, S.L., Herner, J.D., 2014. Verifying emission reductions from heavy-duty diesel trucks operating on Southern California freeways.

Environ. Sci. Technol. 48 (3), 1475–1483.
Kumar, P., Pirjola, L., Ketzel, M., Harrison, R.M., 2013. Nanoparticle emissions from 11 non-vehicle exhaust sources - a review. Atmos. Environ. 67, 252–277.
Lai, C.H., Chuang, K.Y., Chang, J.W., 2013. Characteristics of nano-/ultrafine particle-bound PAHs in ambient air at an international airport. Environ. Sci. Pollut. Res. 20 (3), 1772–1780.
Larson, T., Henderson, S.B., Brauer, M., 2009. Mobile monitoring of particle light absorption coefficient in an urban area as a basis for Land use regression. Environ. Sci. Technol. 43 (13), 4672–4678.
Liati, A., Brem, B.T., Durdina, L., Vögtli, M., Arroyo Rojas Dasilva, Y., Dimopoulos Eggenschwiler, P., Wang, J., 2014. Electron microscopic study of soot particulate matter emissions from aircraft turbine engines. Environ. Sci. Technol. 48 (18), 10975–10983.
Lobo, P., Hagen, D.E., Whitefield, P.D., 2012. Measurement and analysis of aircraft engine PM emissions downwind of an active runway at the Oakland International Airport. Atmos. Environ. 61, 114–123.
Lobo, P., Hagen, D.E., Whitefield, P.D., Raper, D., 2015. PM emissions measurements of in-service commercial aircraft engines during the Delta-Atlanta Hartsfield Study. Atmos. Environ. 104, 237–245.
Masiol, M., Harrison, R.M., 2014. Aircraft engine exhaust emissions and other airport-related contributions to ambient air pollution: a review. Atmos. Environ. 95, 409–455.
Masiol, M., Harrison, R.M., 2015. Quantification of air quality impacts of London heathrow airport (UK) from 2005 to 2012. Atmos. Environ. 116, 308–319.
Park, S.S., Kozawa, K., Fruin, S., Mara, S., Hsu, Y.-K., Jakober, C., Winer, A., Herner, J., 2011. Emission factors for high-emitting vehicles based on on-road measurements of individual vehicle exhaust with a mobile measurement platform. J. Air & Waste Manag. Assoc. 61 (10), 1046–1056.
Payne, M.K., Joseph, E., Sakai, R., Fuentes, J.D., Stockwell, W.R., 2014. Meteorological controls on particle growth events in Beltsville, MD. USA during July 2011 J. Atmos. Chem. 72 (3), 423–440.
Preble, C.V., Dallmann, T.R., Kreisberg, N.M., Hering, S.V., Harley, R.A., Kirchstetter, T.W., 2015. Effects of particle filters and selective catalytic reduction on heavy-duty diesel drayage truck emissions at the port of Oakland. Environ. Sci. Technol. 49 (14), 8864–8871.
Riley, E.A., Banks, L., Fintzi, J., Gould, T.R., Hartin, K., Schaal, L., Davey, M., Sheppard, L., Larson, T., Yost, M.G., Simpson, C.D., 2014. Multi-pollutant mobile platform measurements of air pollutants adjacent to a major roadway. Atmos. Environ. 98 (0), 492–499.
Starik, A.M., Lebedev, A.B., Savel'ev, A.M., Titova, N.S., Leyland, P., 2013. Impact of operating regime on aviation engine emissions: modeling study. J. Propuls. Power 29 (3), 709–717.
Timko, M.T., Fortner, E., Franklin, J., Yu, Z., Wong, H.W., Onasch, T.B., Miake-Lye, R.C., Herndon, S.C., 2013. Atmospheric measurements of the physical evolution of aircraft exhaust plumes. Environ. Sci. Technol. 47 (7), 3513–3520.
Unterstrasser, S., Paoli, R., Sölch, I., Kühnlein, C., Gerz, T., 2014. Dimension of aircraft exhaust plumes at cruise conditions: effect of wake vortices. Atmos. Chem. Phys. 14 (5), 2713–2733.
Vu, T.V., Delgado-Saborit, J.M., Harrison, R.M., 2015. Review: Particle number size distributions from seven major sources and implications for source apportionment studies. Atmos. Environ. 122, 114–132.
Westerdahl, D., Fruin, S.A., Fine, P.L., Sioutas, C., 2008. The Los Angeles International Airport as a source of ultrafine particles and other pollutants to nearby communities. Atmos. Environ. 42 (13), 3143–3155.
Woo, K.S., Chen, D.R., Pui, D.Y.H., McMurry, P.H., 2001. Measurement of Atlanta aerosol size distributions: observations of ultrafine particle events. Aerosol Sci. Technol. 34 (1), 75–87.
Zhu, Y.F., Fanning, E., Yu, R.C., Zhang, Q.F., Froines, J.R., 2011. Aircraft emissions and local air quality impacts from takeoff activities at a large International Airport. Atmos. Environ. 45 (36), 6526–6533.